

Controlled lateral and perpendicular motion of atoms on metal surfaces

A. Buldum and S. Ciraci

Department of Physics, Bilkent University, Bilkent 06533, Ankara, Turkey

(Received 14 November 1995)

We present the theoretical study of the controlled lateral and perpendicular motion of Xe on the Pt(111) surface. The lateral translation of Xe is manipulated by a tungsten tip of a scanning tunneling microscope. Using molecular statics and dynamics the energetics and different modes of atom translation are revealed. In the controlled and reversible transfer of Xe between two flat Pt(111) surfaces, effective charge on Xe, and the dipole moment of the Xe-Pt bond, are calculated as functions of the Xe-surface separation. The contributions of various mechanisms to the transfer rate of Xe are investigated by using the calculated quantum states of Xe under the applied bias voltage. These are tunneling and ballistic transfer, dipole excitation and excitation due to resonant tunneling of electrons, and electron wind force. We found that a single power law for the transfer rate does not exist in the whole range of applied pulse voltage. At high pulse voltage the transfer rate is dominated by the inelastic electron tunneling. At low pulse voltage the rate due to thermally assisted tunneling and ballistic transfer becomes important. [S0163-1829(96)03527-8]

I. INTRODUCTION

Recent developments made in scanning tunneling microscopy (STM), such as translation and relocation,¹ controlled diffusion,² desorption and dissociation of atoms at surfaces,^{3,4} and reversible transfer of atoms between tip and sample surface,⁵ have demonstrated that the manipulation and modification of matter on the atomic scale is now possible. While surface physics has made tremendous progress related to static interactions of various surfaces with adsorbed atoms or molecules for two decades, the controlled motion of adsorbed species has opened a new field of research with interesting physics and perhaps with future potential applications.⁶ The effects of tip-sample interaction on the electronic and atomic structure at close proximity to the tip have been the subject of earlier studies.^{7,8} Here, the tip-atom-surface interaction modifies the potential energy and may introduce new local minima for the adsorbate on the Born-Oppenheimer surface for a given position of the tip. Usually these minima follow the motion of the tip. External agents, such as external electric field, photons, and electrons can influence the controlled dynamics of atoms. In the course of the controlled motion the adatom can be also transferred from sample to tip. The idea that an atom can be transferred between the tip and sample surface is due to Gomer.⁹ The potential energy of the adsorbate between tip and sample surface (or between two electrodes) forms a double-well structure; the energy barrier between wells is crucial for the atom transfer. The atom transfer is simply the crossing of the potential barrier between two wells. This barrier is modified by changing the tip-sample separation and/or by applying a voltage pulse. Earlier, the variation of the double-well potential corresponding to open- and closed-shell atoms between two metal surfaces has been investigated from first principles.¹⁰

The mechanisms responsible for the controlled motion of atoms by STM have been treated recently. Some studies have investigated the lateral translation of inert gas atoms adsorbed on the metal surfaces by using *ab initio*¹¹ and em-

pirical potentials.^{12,13} The dynamics and different modes of lateral motion on the metal surface are now well understood. The mechanism of transfer between two electrodes is known for strongly bound atoms, such as a Si atom between a Si surface and a tungsten tip³ or a Au atom between gold electrodes.⁴ However, the physical phenomena involved in the reversible transfer of Xe between the Ni surface and W tip (so-called atom switch) have not been clarified yet. Eigler, Lutz, and Rudge⁵ found power-law dependence of the transfer rate on the pulse voltage according to $V^{4.9}$ and proposed heating assisted electromigration as the mechanism consistent with their observations. However, the power-law dependence has been disputed and different mechanisms are put forward to explain the reversible transfer in recent theoretical studies.¹⁴⁻¹⁸ The key issues to be resolved are now the verification of the power-law dependence and the clarification of the role of different mechanisms in the transfer rate for a different range of applied pulse voltage.

It is clear that the form of the double-well potential, especially the height and width of the energy barrier, are crucial for the transfer of Xe. The energy barrier, in turn, depends on the form of the empirical potential. Moreover, the variation of the height of the barrier under the pulse voltage is strongly dependent on the excess charge of Xe. Similarly, the variation of the dipole moment of the Xe-Pt bond is important for the vibrational excitation of the adatom.

This work presents the theoretical study of the controlled lateral and perpendicular motion of a Xe atom on the Pt(111) surface, for which the interaction between Xe and Pt atoms can be accurately represented by an empirical potential due to Barker and Rettner.¹⁹ This potential is consistent with a wide range of dynamical and equilibrium data and yields that the equilibrium position of the single Xe atom lies directly above a surface platinum atom. Recently, a self-consistent-field (SCF) cluster calculation²⁰ indicated also the top site as the adsorption position of Xe on the Pt(111) surface. For lateral motion we used a W(111) tip and examined the potential energy surface, which is essential for the dynamics of adatom. Further, in regard to earlier experiments and the

simulations related with the lateral translation of Xe on the Ni(110) surface, the present results clarify the role of surface structure, adsorption site, and material parameters.

The study of the perpendicular motion of Xe is carried out between two flat Pt(111) slabs. This way we simplify the problem by eliminating some unknown factors existing in the transfer process. For example, we do not deal with the uncertainties due to the effect of the adsorption site and tip structure. The objective of this paper is to provide appropriate treatments for the effective charge of Xe and the dipole moment of the Xe-Pt bond, and to reveal the contributions of various mechanism in the transfer rate.

II. LATERAL TRANSLATION OF Xe ON Pt(111)

The interaction energy between xenon and the Pt(111) surface consists of (i) short-range and attractive interaction energy due to the charge rearrangements in the chemical bond, (ii) short-range repulsive energy, (iii) long-range and attractive van der Waals energy. It is usually argued that the charge rearrangement upon physisorption of closed-shell atoms, such as Xe on metal surfaces, is negligible, and hence does not induce any short-range attractive interaction. On the contrary to this argument, the local density treatment of the interaction between closed-shell atoms and jellium metal surfaces by Lang²¹ provided a good account of experimental data on atomic binding energy, dipole moment, and core-level binding energy shift. By examining work-function measurements of rare-gas atoms adsorbed on metal surfaces Ishi and Viswanathan²² concluded that the chemical binding effects are essential in bonding. Recently, Baratoff, Ciraci, and Stoll¹¹ carried out a self-consistent field pseudopotential calculation with the local density approximation for the binding energy of Xe on the Al(111) surface. The calculated binding energy was 130 meV, which is compared to the experimental binding energy of 200 meV. This indicates that even for the adsorbed closed-shell atoms the short-range interaction near the equilibrium distance dominates the weak long-range interaction. The free parameter linear combination of atomic orbitals (LCAO) calculation by Pérez *et al.*²³ also confirms this conclusion.

In the present calculations of lateral motion the Pt surface is represented by 42 Pt(111) atomic layers comprising 14 112 Pt atoms. The tip is constructed by 2024 W atoms in pyramidal geometry generated from 22 W(111) layers. The apex of the tip has a single atom; the second layer has three atoms. The coordinates of the tip (apex atom) and those of Xe relative to a point on the sample surface are labeled by (x, y, z) and (ξ, κ, ζ) , respectively. The interaction potential between the Xe atom (at \mathbf{R}_a) and any atom of the W tip (at \mathbf{R}_i) is expressed in terms of a Lennard-Jones pair potential having the well-known form $\epsilon[(r_0/|\mathbf{R}_a - \mathbf{R}_i|)^{12} - 2(r_0/|\mathbf{R}_a - \mathbf{R}_i|)^6]$. The parameters of this potential are determined¹³ from the experimental data to be $\epsilon = 0.339$ eV, and $r_0 = 3.62$ Å. The many-body effects are taken into account by scaling ϵ and r_0 values. Note that the Lennard-Jones pair potential function is only a crude approximation for the Xe-W interaction; it could have been improved by using additional terms. This, however, requires additional experimental data to fit, which are not available yet. The atomic arrangement of the tip-atom-surface system and the

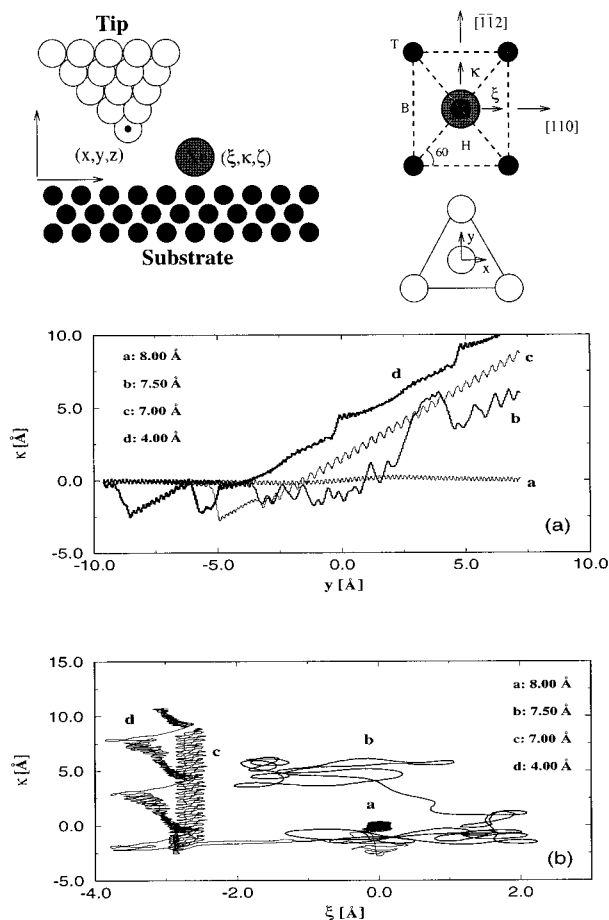


FIG. 1. Lateral translation of Xe on the Pt(111) surface induced by the W tip moving along the $y[\bar{1}\bar{1}2]$ direction. a , b , c , and d correspond to different heights z of the tip. Trajectories of Xe in the (κ, y) and (κ, ξ) planes are shown in the top and bottom panels, respectively. The direction and orientation of the tip relative to the Pt(111) unit cell are shown schematically.

orientation of the tip are schematically described in Fig. 1.

The empirical potential introduced by Barker and Rettner¹⁹ expresses the interaction between a single Xe atom and the Pt(111) surface in terms of the sum of nonspherical, pairwise additive potentials and of an additional term, which describes the interaction of Xe with the delocalized conduction electrons of the sample surface. The nine parameters in the potential function were fitted to a wide range of available experimental data. Details of this potential can be obtained in Ref. 19.

The electrodes [i.e., the W tip and the Pt(111) substrate] are taken rigid. As a result, the position of atoms in these electrodes are fixed at their bulk equilibrium positions and hence part of the interatomic interactions (such as Pt-Pt, Pt-W, and W-W) are not taken into account in the total potential function. The assumption of rigid electrodes is valid if the height z of the tip is large. For relatively smaller tip-sample separations the modification of the atomic structure at close proximity to the tip (such as elastic or plastic deformation, wetting, and surface melting) has to be taken into account, however.¹³

The potential energy surface of Xe is calculated at each

TABLE I. Energetics of Xe on the Pt(111) surface. T , H , B denote for top, hollow, and bridge sites, respectively.

	Binding energy E_b (meV)		Barrier energy Q (meV)
H site	222	$T \rightarrow H \rightarrow T$	32
T site	254	$T \rightarrow B \rightarrow T$	26
B site	228		

grid point (ξ, κ) on the Pt(111) surface by varying its height ζ . Then, the potential energy surface is obtained by plotting the minimum values of the calculated energy at each grid point. The highest binding energy (or lowest potential energy) is $E_b = 254$ meV and occurs at the top site. This is in contrast to many adsorbate-substrate systems [such as Xe on the Al(100) surface] in which the hollow site occurs as the equilibrium binding site. The change of the adsorption site on the Pt surface is attributed to the reduction of $s + p$ electron density due to the d states occupied near the Fermi level.²³ The binding energy at the symmetry points of the unit cell and the energy barriers for different directions of motion are shown in Table I.

The potential energy surface is strongly modified by a W tip approaching the physisorbed Xe atom. The minimum of the potential energy, which is displaced towards the tip, usually follows the motion of the tip, if the tip-sample distance is properly varied in the course of translation. The carriage of Xe on the Pt(111) surface as a function of the height of the tip z is studied by performing molecular dynamics calculations. The results for the tip moving along the y direction from a distance towards Xe at different heights z are summarized in Fig. 1. The tip moves from a distance towards Xe for different values of z . For $z = 8 \text{ \AA}$, the Xe atom remains practically unaffected. At $z = 7.5 \text{ \AA}$, the interaction between the tip and Xe becomes significant; first it is attracted by the motion of the tip, then it follows the tip for a very short distance, but then it becomes unaffected by the tip. For $5 \text{ \AA} < z < 7 \text{ \AA}$, Xe is attached to the tip and is then carried without showing any periodicity due to the surface corrugation. For this range of z the interaction sets in already at $\kappa - y = 5 \text{ \AA}$ since the second layer of tip atoms is closer to Xe; the Xe atom escapes $\sim 2.7 \text{ \AA}$ sideways to the adjacent unit cell and at the same time is attached to the side face of the W tip. Only for a smaller height of the tip ($z < 5 \text{ \AA}$) is the corrugation of the Pt(111) surface reflected to the trajectory of Xe. In this case, Xe escapes again sideways by $\sim 2.7 \text{ \AA}$ to the adjacent top site and pushed by the tip moving along the $[\bar{1}\bar{1}2]$ direction. The jumps of the curve d in the upper panel correspond to the Xe atom from one T site to the next one along the $[\bar{1}\bar{1}2]$ direction. In the bottom panel of Fig. 1 we show the (κ, ξ) trajectories of Xe corresponding to the same set of z in panel (a). The Xe atom carried by the tip at $z = 7 \text{ \AA}$ traces a straight route along the κ axis with ξ fixed at $\sim 2.7 \text{ \AA}$. For $z = 4 \text{ \AA}$, the zigzag trajectory is produced by Xe, which is pushed from one T site to the next one along the $[\bar{1}\bar{1}2]$ direction by avoiding the H site. This behavior of pushing mode is rather different from that found in the controlled motion of Xe on the Ni(110) surface.^{12,13}

The translation of Xe along the $[110]$ direction (or x di-

rection) is similar to the one along the $[\bar{1}\bar{1}2]$ direction described above. The energy barrier in the lateral motion of Xe on the Pt(111) surface is smaller than that on the Ni(110) surface. This is because the Pt(111) surface is a closed-packed plane and the surface charge density has relatively smaller corrugation. Due to this fact the lateral translation of Xe on the surface exhibits the periodicity of the substrate only in a certain range of z . The trajectories presented in Fig. 1 are closely related to the two-dimensional stick-slip motion in the science of friction. The energy damping from this motion is of current interest.

III. REVERSIBLE TRANSFER OF Xe BETWEEN FLAT Pt(111) ELECTRODES

The atom transfer between two electrodes has been realized for weakly as well as strongly bound adsorbates. Mamin, Guethner, and Rugar⁴ achieved the transfer of gold atom from a negatively biased gold tip to a substrate. They argued that negative Au-ion formation and subsequent field evaporation is responsible for the transfer. Lyo and Avouris,³ who realized reversible atom transfer between the tip and Si substrate, have suggested that the transfer takes place by ionization (positive Si-ion formation) followed by field evaporation. The controlled and reversible transfer of the weakly bound Xe atom between the Ni(110) surface and a W tip, so-called atom switch,⁵ displayed characteristics that are quite different from the two former cases.^{3,4} For example, (i) Xe is always transferred towards the positively biased electrode. (ii) At small tip-sample distance (corresponding to the junction resistance $R < 700 \text{ k}\Omega$) the Xe atom moves spontaneously to the tip without the need to apply a positive pulse voltage. (iii) At larger separation ($R > 1.5 \text{ M}\Omega$), however, Xe either hops on the Ni surface or escapes from the junction entirely. (iv) Depending upon the location of the Xe atom [at kink sites, on the bare Ni(110) terrace, on top of a single Ni adatom on the Ni(110) surface] the conductance ratio ranges from unity to 7. (v) There is a characteristic transfer rate for a fixed sample distance. For example, it is claimed⁵ that for a $906\text{-k}\Omega$ junction the transfer rate has a power-law dependence on the pulse voltage, according to $\tau^{-1} \approx V_p^{4.9 \pm 0.2}$. Gao, Persson, and Lundqvist¹⁴ examined various physical mechanisms responsible for the reversible transfer of Xe between the Ni(110) surface and a W tip, and proposed vibrational heating by inelastic electron tunneling to explain the power-law dependence reported by Eigler, Lutz, and Rudge.⁵ They also concluded that the multiple (incoherent) vibrational excitation via inelastic electron tunneling plays an important role. Later, Salam, Persson, and Palmer¹⁷ argued that for other systems, such as Na on Cu, the coherent multiple excitation of the adsorbate-substrate bond caused by inelastic

tunneling of a single electron (or hole) via negative (or positive) ion resonance dominates the vibrational heating (incoherent excitation). They found the vibrational heating mechanism to dominate over the coherent mechanism in the case of the atom switch.⁵ On the other side, Saénz and Garcia¹⁵ proposed that the experimentally observed atom transfer process⁵ complies with a thermally assisted single-atom tunneling. They argued that the transfer rate cannot follow a power-law dependence with the applied pulse at small voltages. Moreover, they were able to reproduce the observed dependence of the transfer rate on the applied pulse at the high voltage region only by using unrealistically large and constant (and negative) effective charge ($q_{\text{eff}}=0.3e$) on the physisorbed Xe atom.

A. Variation of potential energy of Xe

The potential energy of Xe between two flat Pt(111) surfaces separated by z is $U(\xi, \kappa, \zeta, z; V_p)$ and has double minima for $z > 2\zeta_0$ [ζ_0 being the equilibrium distance of Xe adsorbed on the Pt(111) surface]. Two wells (each being closer to one of the Pt surfaces) determine the equilibrium distance and energy of Xe between two electrodes but adsorbed only to one of them. As z decreases the energy barrier $Q(z)$ is lowered and eventually collapses, leading to a single well. Since we are interested in the motion along ζ , we adopt a one-dimensional model and consider only the variation of U along the [111] direction. Implementation of the other directions would bring new eigenstates, which do not play a crucial role in the transfer rate. For the system used in the present study $U(\zeta, z)$ is symmetric in the absence of applied bias voltage.

We generate the potential (energy) function $U(\zeta, z)$ of Xe between two parallel and flat Pt(111) electrodes by using Barker and Rettner¹⁹ potential described in Sec. II. At relatively small z , this potential gives us a shallow well at the center in addition to two deep wells. It occurs perhaps due to the limitation of the interpolation between the short-range and the long-range part of the potential function. If this were the real situation, the resonant tunneling of atoms would occur across the wells in appropriate conditions. This artifact of the potential is corrected by improving the interpolation between two ranges of the interaction. In Fig. 2 we illustrate the potential energy curves along the [111] direction (or the ζ direction) for different separation z , and variation of Q with z . The symmetry of $U(\zeta, z)$ is broken by applying a pulse voltage if the adsorbed Xe is charged and/or the Xe-Pt bond is polarized. In this case one well is lowered relative to the other, and also the energy barrier is decreased. This way not only the directionality but also the control of Xe transfer becomes possible.

Apparently, the effective charge of the adsorbed Xe as well as the charge distribution of the Xe-Pt bond are two features that are critical ingredients of the atom transfer. The physisorption of Xe on simple metals as well as on transition metals results in the reduction of the work function^{22,24} Φ . This is ~ 0.96 eV for the density of $\sim 6 \times 10^{14}$ Xe atoms per cm^2 on a platinum²⁴ surface. This implies that the Xe-Pt bond induces a dipole moment that is in the reverse direction to that of the bare surface. The dipole moment leading to the work function lowering $\Delta\Phi \approx -0.96$ eV is determined by

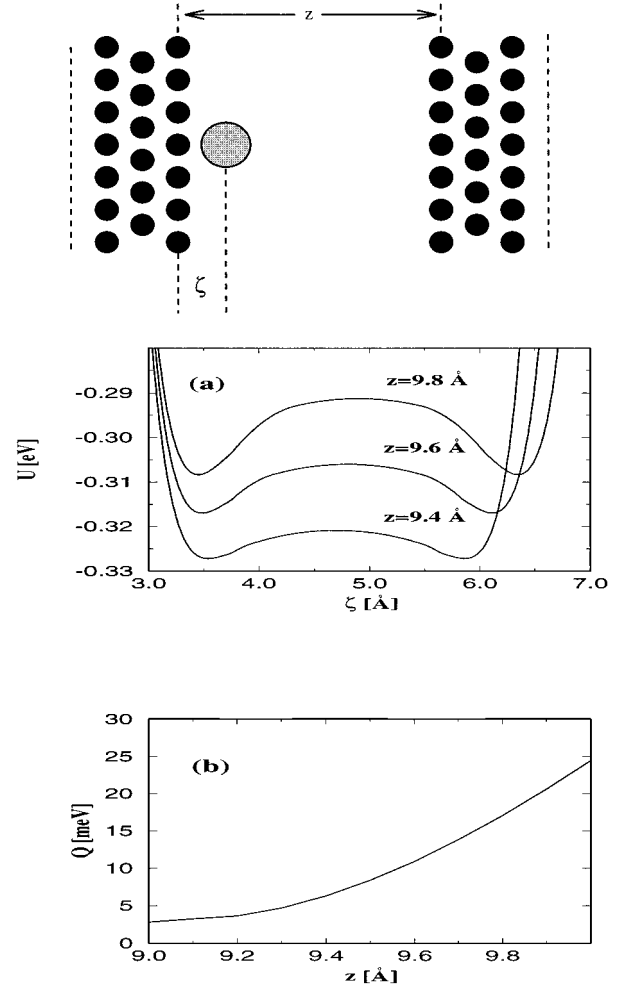


FIG. 2. (a) Variation of the potential energy of Xe, $U(\zeta, z)$, with the separation of the Pt(111) electrodes z . (b) Variation of the barrier energy $Q(z)$ with separation. The bias voltage $V_p=0$. The arrangement of electrodes and the relevant coordinates are described schematically.

using Topping's formula²⁵ to be 0.65 D. The character and charge distribution of the bond between an adsorbed inert gas atom and the metal surface have been the subject of several studies. Unfortunately, theoretical results reported to date are not conclusive. A recent local density approximation calculation by Müller²⁰ suggests that the Xe $5p$ orbital makes bonding and antibonding combinations with occupied metal states. On the other hand, as a result of the combination of the Xe $5p$ state and partially filled Pt $5d$ state, the charge $\Delta q=0.085$ electrons is transferred from Xe to the metal. This provides the binding by lowering the Xe $5p$ level by $\Delta q(E_F - \epsilon_{\text{Xe}5p})$. Clearly, the local bonding and the charge transfer are usually emphasized in the cluster calculations.²⁰ Based on the atom-on-jellium calculations, Eigler *et al.*²⁶ proposed that the empty Xe $6s$ level, which lies above the Fermi level, is broadened upon the adsorption of Xe on the metal surface and becomes partially occupied. Hence, the finite local density of states at the Fermi level, $\rho(r, E_F)$ renders Xe visible in the STM. The existence of this so-called s -resonance model for Xe adsorbed on the metal surfaces was suggested several years ago.²⁷ Clearly, the par-

tial occupation of the Xe 6s resonance by the metal electrons indicates the charge transfer from the metal to the adsorbed Xe. Such a broadening of the empty adsorbate level does not occur in a metal cluster consisting of a few metal atoms as in the model of Müller.²⁰

The charge transfer of Xe is in agreement with the findings of the SCF pseudopotential calculation.¹¹ The free-parameter LCAO calculation by Pérez *et al.*²³ also finds that charge is transferred from the Al(100) surface to the adsorbed Xe to yield $q_{\text{eff}} \sim 0.1$ electron. Experimentally, Wandelt and Gumhalter²⁸ found direct support from the ultraviolet photoemission spectroscopy of the valence band of the Xe-covered Pd surface that the Xe 6s resonance is partially occupied and the physisorbed Xe becomes negatively charged.

The partial filling of the Xe 6s resonance leading to a charge transfer to the adsorbed Xe is estimated²⁹ by using the chemisorption theory³⁰ based on Anderson's Hamiltonian³¹ where the states of the metal-adatom system $|\phi\rangle$ are expanded in terms of the adatom $|a\rangle$ and metal $|k\rangle$ states. Then the density of states localized in a particular adatom state $|a\rangle$ is $\rho_a(\epsilon) = \sum_{\phi} |\langle \phi | a \rangle|^2 \delta(\epsilon - \epsilon_{\phi})$. This is formulated³⁰ as

$$\rho_a(\epsilon) = \frac{\Gamma}{\pi} [(\epsilon - \epsilon_a - \Lambda)^2 + \Gamma^2]^{-1}, \quad (1)$$

which is approximately centered at $\epsilon = \epsilon_a + \Lambda$ and has half width at half maximum Γ . It is seen that the empty state of a free Xe atom is broadened and displays a Lorentzian-like distribution upon adsorption on a metal surface. The tail of this resonance dips in the Fermi level and becomes partially occupied. That is $n = 1/2 - \pi^{-1} \arctan(\epsilon/\Gamma)$. In the present case Γ is expressed as

$$\Gamma \approx \pi \left| \langle \psi_{\text{Xe}6s} | \psi_{\text{Pt}6s} \rangle \frac{\epsilon_{\text{Xe}6s} + \epsilon_{\text{Pt}6s}}{2} \right|^2, \quad (2)$$

where the local overlap $\langle \psi_{\text{Xe}6s} | \psi_{\text{Pt}6s} \rangle$ is calculated numerically by using the Herman-Skillman³² wave function and is found ~ 0.44 for the equilibrium adatom-substrate distance, $\zeta = \zeta_0$. Since the spin-polarized electron spectroscopy³³ sets the position of the $\epsilon_{\text{Xe}6s}$ level, $\epsilon_a + \Lambda$, 3.91 eV above the Fermi level, the partial filling of the Xe 6s resonance is found to be 0.08 per spin at the equilibrium distance ζ_0 of the adsorbed Xe. Note that the occupation of the Xe 6s resonance varies with the distance ζ between Xe and the Pt(111) surface in the course of the transfer. The effective charge of Xe between two Pt(111) electrodes, $q_{\text{eff}}(\zeta, z)$ is estimated by adding the excess charge on Xe originating from each electrode, $\Delta q(\zeta)$ and $\Delta q(z - \zeta)$. Of course, the additivity of Δq associated with each electrode is justifiable only for relatively large z . At small z , the interelectrode interaction has to be taken into account. Figure 3 illustrates the variation of the effective charge $q_{\text{eff}}(\zeta, z)$ for a given z . Finally, because of q_{eff} the potential energy $U(\zeta, z)$ is modified under the applied pulse voltage V_P . That is

$$\Delta U(\zeta, z; V_P) = -q_{\text{eff}}(\zeta, z) \frac{\zeta - d_i}{z - z_i} V_P, \quad (3)$$

where d_i is the image plane position³⁴ for the first atomic plane of the electrode and $z_i = 2d_i$. Figure 4(a) illustrates the

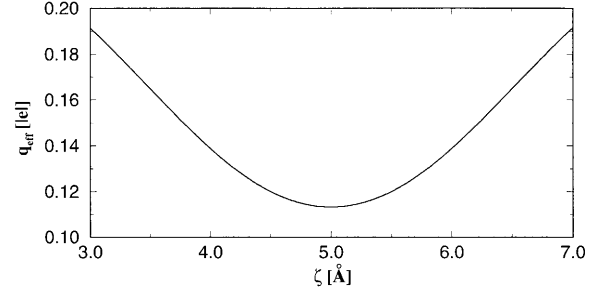


FIG. 3. Variation of the effective charge $q_{\text{eff}}(\zeta, z)$ on Xe between two Pt(111) electrodes separated by $z = 10.0$ Å.

variation of the potential energy with different applied pulse voltages. Note that for a given z and V_P , ΔU decreases linearly and reduces the barrier only when q_{eff} is constant. However, the variation of the barrier with ζ is not obvious if the value of the q_{eff} varies with ζ . For example, for $\Delta q(\zeta) \sim e^{-\beta\zeta}$, Q increases for $\beta > 0.88$, but decreases for $\beta \leq 0.88$ for $z = 10$ Å. In Fig. 4(b), the variation of $Q(z; V_P)$ is shown for calculated $q_{\text{eff}}(\zeta, z)$, as well as for constant q_{eff} . Note that the barrier lowering with V_P becomes dramatic if q_{eff} is taken constant. In view of the present results, earlier conclusions based on the constant q_{eff} are seriously questioned.

The change of U with V_P , and hence the directionality of atom transfer, can also be obtained from the adsorption-induced dipole²³ as done by Walkup, Newns, and Avouris.¹⁶

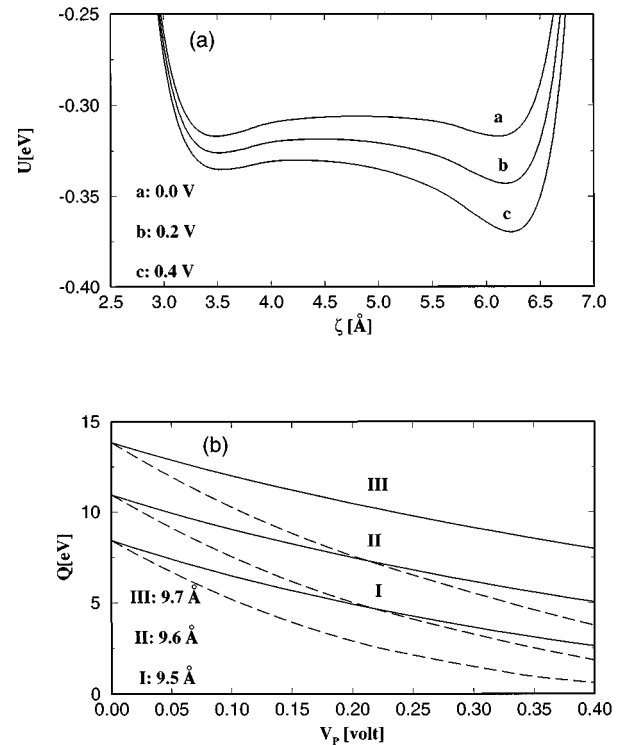


FIG. 4. (a) Variation of the potential energy $U(\zeta, z; V_P)$ of Xe between two Pt(111) electrodes with different applied bias voltage V_P for $z = 9.6$ Å. (b) Variation of the energy barrier $Q(z; V_P)$ with applied bias voltage V_P for three different electrode separations z (I, II, III). The dashed curves correspond to $Q(z; V_P)$ where $q_{\text{eff}}(\zeta, z)$ is constant and equals 0.16 electron.

The dipole takes on opposite signs for adsorption on the sample and tips, and it provides the observed directionality of the Xe motion. The calculation of dipole moment, however, requires that the distribution of charge at the Xe-adsorbed semi-infinite Pt surface is obtained self-consistently. Yet such a calculation is not available. In our approach we calculate $\Delta U(\zeta, z; V_p)$ by using q_{eff} which is obtained unambiguously from the chemisorption model.^{30,31} A similar model in a much simpler and parametrized form was used by Saénz and Garcia.¹⁵ Both approaches used in calculating ΔU (i.e., one due to Walkup, Newns, and Avouris¹⁶ and one used here) are acceptable and interrelated. We note that the excess charge on Xe due to the $6s$ resonance (which is also crucial for the STM image of Xe) does not contradict the lowering of the work function as a result of Xe adsorption. The dipole moment leading to the work-function lowering is obtained from the integration of the charge near the surface, and hence even a slight polarization of charge on Xe may induce significant dipole moment. The dipole moment μ of the Xe-Pt bond that lowers the work function is made from three major components,²⁸ namely,

$$\mu = \mu_s + \mu_d + \mu_q. \quad (4)$$

These are, respectively, static polarization, dynamic polarization, and charge transfer components. Here, $\mu_s + \mu_d$ and μ_q are competing contributions. While the work function is reduced by $\mu_s + \mu_d$, μ_q , which has the opposite sign of $\mu_s + \mu_d$, raises Φ . The origin and the character of these components are extensively discussed and contrasted with reverse face specificity of Φ and adsorption energy by Wandelt and Gumhalter.²⁸ They even pointed out experimental work on the Cs surface, where the adsorption of Xe having $\mu_q > \mu_s + \mu_d$ leads to an increase of Φ .

As in $q_{\text{eff}}(\zeta, z)$, the variation of μ with the distance from the metal surface is also needed in the study of atom transfer. μ_q varies as q_{eff} does, since it is equal to $2\bar{d}_i q_{\text{eff}}$. Here $\bar{d}_i = \zeta - d_i$. As for μ_s we assume the form $\mu_s = CS\bar{d}_i$ in terms of the overlap S between Pt $5d_{20}$ and Xe $5p_z$ orbitals and constant C to be fitted to the equilibrium value. For $\bar{d}_i = 1.288 \text{ \AA}$, $S = 0.055$, $C = 3.75 \times 10^{-9}$ esu, and $\partial\mu/\partial\zeta = 0.835D/\text{bohr}$.

At a preset electrode separation, the atom transfer can be viewed as the crossing of the barrier, which is momentarily reduced by V_p . In the asymmetric potential $U(\zeta, z; V_p)$ the Xe atom can have certain quantum states $\Psi_n(\zeta, z; V_p)$ with energies $E_n(z, V_p)$ and frequency $\omega_n(z, V_p)$ ($n=0, 1, 2, \dots$), which are obtained from the numerical solution of the Schrödinger equation. Here the state $n=0$ denotes the ground state. The bound states are localized in one of the wells. States having energy above the barrier may have comparable weights on both sides. The Xe atom, which is initially trapped in one of the wells, becomes excited and is transferred to the other well (by tunneling and ballistic process) and is relaxed. In what follows different processes (or mechanisms) contributing to the transfer rate at a given z and V_p are investigated.

B. Thermally assisted transfer of Xe

As substantiated by the experiment,⁵ the Xe atom can move spontaneously from one electrode, where it is initially

bound to the other one by tunneling even for $V_p=0$. Of course, for Xe of mass M the transmission probability T across an energy barrier of significant height and width is negligible. However, by decreasing the electrode separation z the height of the energy barrier for adsorbed Xe is decreased. This may result in a significant transfer rate. The tunneling barrier for the Xe atom at the i th quantum state localized on one of the electrodes is $\phi_i = Q - E_i(z, V_p)$. The thermal probability of Xe to be at the i th state at temperature T is $P^i(T) = e^{-E_i/k_B T} / \sum_j e^{-E_j/k_B T}$ where the summation index j runs over all localized states on the same site of Xe. The transmission probability T_i for the state Ψ_i is less than unity for $\phi_i > 0$, but becomes unity if $\phi_i \leq 0$ or E_i lies above the barrier. The latter corresponds to the ballistic transfer of Xe.

As seen in Fig. 4(a), the applied pulse voltage V_p induces asymmetry in the potential energy, which is otherwise symmetric for the system at hand. The eigenstates for the Xe atom are modified; while the well near the (left) electrode where the Xe is initially bound has fewer states, the (right) well at the other side (where the positive bias is applied) becomes deeper and has more eigenstates. Normally, the lowest eigenstate of the right electrode is lower than the lowest state of the left electrode. Consequently, an atom that is in thermal equilibrium at the left side is in a nonequilibrium state after it is transferred to the right side, but it is equilibrated quickly by the dissipation of its energy. Energy of Xe is dissipated by the excitation of the electron-hole pair, and mainly by the creation of metal phonons in the electrode. Using the elastic continuum model, we estimate the lifetime of the first excited state $\tau_r \approx 20$ ps for $z = 9.6 \text{ \AA}$ and $V_p = 0.1$ V (see also Refs. 16 and 35) and treat higher states, $\Psi_{n>2}$, within the harmonic approximation. As a result the lifetimes of the higher-lying states decrease with $1/n$. The lifetime of an excited state of a few quantum numbers higher than the ground state becomes less than one period of Xe. Accordingly, Xe loses its energy just after the first ‘‘collision’’ with the right electrode. The net thermally assisted rate τ_{TB}^{-1} for tunneling and ballistic transmission is given by

$$\tau_{TB}^{-1} = \sum_i [f_i^l \omega_i T_i^l P_i^l(T) - f_i^r \omega_i T_i^r P_i^r(T)]. \quad (5)$$

Here, the first and second terms represent the right-going and left-going rates, respectively. Each term is multiplied by the probability of state f_i to be at the related electrode. $P_i^l(T)$ is the thermal probability of the state i relative to the lowest state of the left electrode, and $P_i^r(T)$ is the thermal probability relative to the lowest state of the right electrode. In Eq. (5) the contribution of the second term is neglected and hence a transfer rate only towards a positively biased electrode is considered in the tunneling process. However, $T_i^r = 1$ for the ballistic transfer (corresponding to $\phi_i \geq 0$) and hence the second term in Eq. (5) is not negligible. In Fig. 5 we show the thermally assisted transfer rates (tunneling and ballistic) calculated at $T = 4$ K for different values of z . We note the following features in this figure. First, the calculated transfer rates $\tau_{TB}^{-1}(z; V_p)$ do not exhibit a power-law dependence. Also, $\tau_{TB}^{-1}(z; V_p \rightarrow 0)$ is finite for unidirectional transfer. For $V_p = 0$, $\tau_{TB}^{-1} \sim 10^{-10} \text{ sec}^{-1}$ at $z = 9.8 \text{ \AA}$, but one transfer may occur in each second at $z \leq 9.5 \text{ \AA}$. This implies

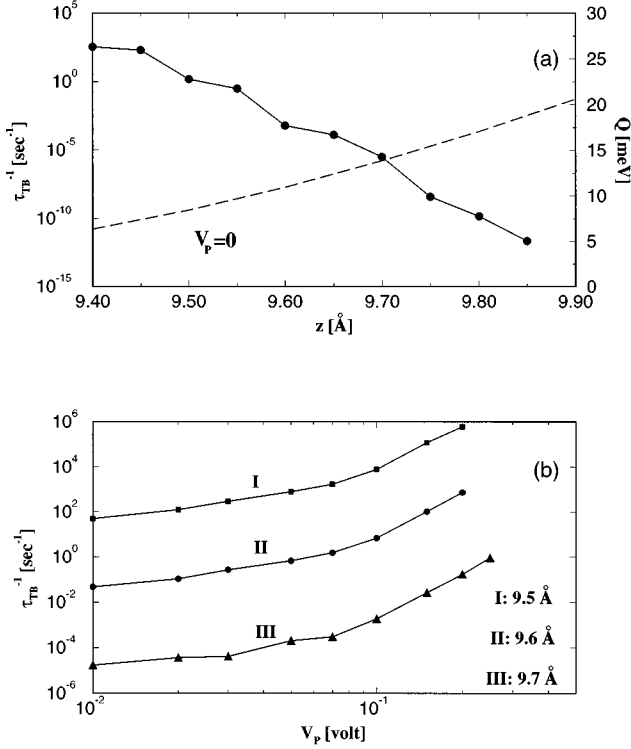


FIG. 5. (a) Rate of thermally assisted (ballistic and tunneling) transfer of Xe (τ_{TB}^{-1}) and potential barriers vs the separation between Pt electrodes, z . (b) Same rate vs V_p for $z=9.5$ Å (I), $z=9.6$ Å (II), and $z=9.7$ Å (III).

that the form of $U(\zeta, z; V_p)$ is extremely important for realistic calculation of the rate of transfer. A potential energy function yielding a sharp barrier may be relatively less sensitive to the variation of z . Second, the variation of the transfer rates with the pulse voltage and especially with the separation z is not smooth. The reason is that there are small numbers of discrete energy states involved in the transfer process. The last energy state below the energy barrier and the first state above the barrier make a dominant contribution to τ_{TB}^{-1} . Modification of potential energy and hence lowering of the barrier with V_p leads to discontinuous changes in the spectrum relative to the energy barrier. This may give rise to discontinuous changes in τ_{TB}^{-1} .

C. Momentum transfer by tunneling electrons

Electrons that tunnel under the applied pulse voltage will be inelastically scattered by the adsorbed Xe atom. In accordance with the ballistic model of the electromigration of Fiks and Huntington,³⁶ tunneling electrons transfer momentum Δp to Xe during the collision process, which in turn induces so-called electron wind force acting on Xe. In this simple picture the energy transfer can be estimated by $(I/e) \times (\Delta p)^2 / 2M$. Walkup, Newns, and Avouris¹⁶ found that the electron wind force is one order of magnitude smaller than the dipole force. Following the approach of Ralls, Ralph, and Buhrman,³⁷ Sáenz and Garcia¹⁵ expressed the temperature rise of Xe due to the energy transfer from the tunneling electrons by $\Delta T \sim CV_p^2$, where C is taken as a constant to be determined from experimental data. The curve $\tau^{-1}(V_p)$ they

calculated for a wide range of C was quite different from the experimental data. It appears that the heating-assisted electromigration (or electron wind force) makes a small contribution to the net transfer rate.

D. Excitations of Xe by inelastic electron tunneling

A small fraction of electrons tunnel inelastically between two electrodes; they transfer energy to the Pt-Xe bond by two different processes: resonant tunneling and dipole excitation. Inelastic electron tunneling through an adsorbate has been treated earlier,^{38–40} and already proposed^{14,16,17} as a mechanism responsible for Xe transfer in the atom switch. In resonant tunneling, the tunneling electron is temporarily trapped in the Xe $6s$ resonance. Owing to increasing excess charge on Xe the potential energy curve (or surface) in Fig. 4(a) is lifted to an excited energy state. In a time interval corresponding to the tunneling time τ_t , the potential energy returns to its initial state, but Xe goes to a higher vibrational excited state, $\Psi_{n>0}$. This process, which is also referred to as the local polaron model, may involve even the Coulomb blockade, and may be quite complicated. A small fraction of tunneling electrons engages also in dipole excitation of the Xe-metal bond. This way the adsorbate may reach an excited vibrational state Ψ_n , for which $E_n \geq Q$, and be ready for transfer across (or over) the barrier. The excited adsorbate can reach this level in a single step (coherent process) created by one-electron tunneling or in multiple steps (incoherent process) created by subsequent tunneling of electrons.¹⁷ It is argued that $\tau_r \geq \tau_t$ makes the (incoherent) multiple vibrational excitation valid both in dipole excitation and the resonant tunneling process for Xe transfer. To calculate the contribution of both processes we use the formalism developed earlier³⁹ and follow the below steps.

To calculate the contribution of resonant tunneling and dipole excitation processes one needs to know the fraction of electrons that engage in the inelastic tunneling. As proposed earlier^{16,39} the fraction of inelastic electrons contributing to dipole excitation from the ground state to the first excited state is approximately $\eta_d = (\langle \psi_1 | \zeta | \psi_0 \rangle \partial \mu / \partial \zeta)^2 (ea_0)^{-2}$, where a_0 is the Bohr radius. We estimate $\eta_d = 2.75 \times 10^{-3}$ for the electrode separation $z = 9.7$ Å. Walkup, Newns, and Avouris¹⁶ estimated the fraction of electrons η_r leading to the resonant tunneling process through the $6s$ state, which lies ~ 4 eV above the Fermi level and has a width of ~ 1 eV. They found $\eta_r \approx 3 \times 10^{-4}$. Then the total fraction of inelastic tunneling is $\eta = \eta_d + \eta_r$ and the number of inelastic electron tunneling events per second is $\beta = (I/e)\eta$.

Based on the arguments above we adopt the (incoherent) single-step process, and within the harmonic approximation the rate of excitation (and also relaxation) from the $n-1$ state to the n state, g_{n-1} (or decay from n to $n-1$, r_n) is larger than that from the ground state to the first excited state by a factor of n . Finally, the master equation for a single-step process reads⁴¹

$$\dot{P}_n = r_{n+1}P_{n+1} + g_{n-1}P_{n-1} - (r_n + g_n)P_n \quad (6)$$

in terms of the occupation probability P_n of state n , r_n , and g_n . Since $g_{n-1} = \beta n$ and $r_n = \alpha n$ with $\alpha^{-1} = \tau_r$ in the harmonic approximation, the steady-state solutions become $P_n \propto (\beta/\alpha)^n$. By disregarding the thermal distribution

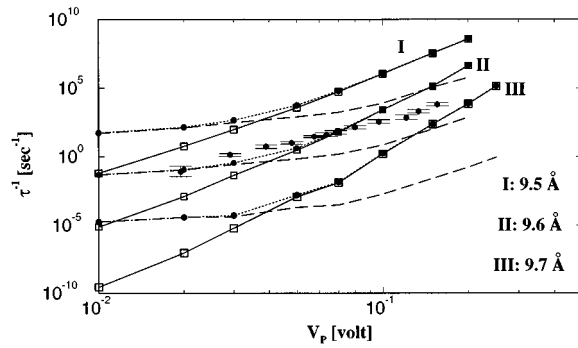


FIG. 6. Transfer rates of Xe vs pulse voltage V_p are calculated for the electrode separation $z=9.5, 9.6,$ and 9.7 \AA . The rate τ_{TB}^{-1} due to the thermally assisted tunneling and ballistic transfer and the rate τ_I^{-1} due to the inelastic tunneling are shown by dashed and continuous lines with squares. The total transfer rate of Xe is illustrated by the dotted curve. The error bars are the experimental data by Eigler, Lutz, and Rudge (Ref. 5) obtained from the rate of transfer of Xe between Ni and W electrodes.

(by taking $T=0$) we calculate the rate τ_I^{-1} of transfer due to the inelastic tunneling. Our results are shown by continuous lines with squares in Fig. 6. Note that this is the rate calculated by Walkup, Newns, and Avouris¹⁶ for the atom switch. As seen the rate $\tau_I^{-1}(V_p; z)$ displays ‘‘approximately’’ a power-law dependence on the pulse voltage. For low V_p , the exponent of the power law is dependent on the electrode separation, but it converges to the same value for high V_p for electrode separation $z \sim 9.6 \text{ \AA}$. We also found that τ_I^{-1} is dependent on the value of the dipole moment and its variation.

E. Total rate of transfer

In order to calculate the total rate of Xe transfer we start with the thermal probabilities $P_n(T)$ of the Xe atom and consider that final steady-state probabilities \mathcal{P}_n are modified by the tunneling current. The steady-state probability of occupation can be obtained from

$$\mathcal{P}_n = \frac{P_n(T)}{F_n} + \sum_{j=0}^{n-1} P_{nj}^D. \quad (7)$$

Here, $F_n = 1 + fc + fc^2 + \dots + fc^{L-n}$, $fc = \beta/\alpha$, and $P_{nj}^D = P_j(T)fc^{n-j}/F_j$. By taking L sufficiently large, new probabilities are determined and are subsequently used in Eq. (5) to calculate the total rate τ^{-1} of transfer (including all contributions). Our results are illustrated in Fig. 6 by dotted curves for different values of z . In the same figure the contributions of thermally assisted tunneling and ballistic transfer are also shown. The experimental data by Eigler, Lutz,

and Rudge⁵ are included for the sake of comparison even if they belong to a different system of electrodes.

IV. CONCLUSIONS

In this work the controlled lateral and perpendicular motions of Xe are investigated. The controlled lateral motion of Xe on the closed-packed (111) surface of Pt is induced by the W tip. The interaction between Xe and the W tip is described by empirical potentials and various modes of motion are revealed depending on the tip-surface separation. The corrugation of the potential energy of Xe is small owing to the closed-packed nature of the metal surface. Consequently, the Xe atom moves more freely as compared to the other surfaces and usually does not follow a straight trajectory in the surface plane. The effect of the tip becomes significant only for the tip separated less than 7.5 \AA . Upon the interaction with the tip, Xe flops first sideways and is carried by the tip for $5 \text{ \AA} < z < 7 \text{ \AA}$, whereas the adsorbed Xe atom is pushed by the tip at smaller separation. The range of z leading to different modes in the controlled motion of Xe depends on the atomic arrangement of the apex of the tip and the tip material. These results are also relevant for boundary lubrication in tribology.

The controlled perpendicular motion of Xe is studied between two flat Pt(111) surfaces. The transfer of Xe is produced by the applied pulse voltage. The present model consisting of two flat electrodes is found suitable to analyze the contribution of various physical processes responsible for the controlled atom transfer since parameters such as tip-structure and tip-material affecting the transfer are not involved. We found that the form of the potential function $U(\xi; z)$, in particular the width of the barrier between two wells, is crucial in determining the contribution of the thermally assisted tunneling and ballistic transfer of Xe. Similarly, the value of the effective charge and its variation with the distance from the surface are important ingredients of the atom transfer. The contribution of electromigration (or electron wind force) in the transfer is known to be small. Our study reveals that the transfer due to thermally assisted tunneling and ballistic transfer of Xe between two Pt(111) electrodes is normally small but becomes dominant for small pulse voltage. Whereas the transfer rate due to the inelastic tunneling of electrons dominates the atom transfer in the range of normal and high pulse voltage. The calculated total rate does not yield a power-law dependence on the applied pulse voltage.

ACKNOWLEDGMENTS

We acknowledge stimulating discussions with Dr. A. Baratoff. This project was partially supported by the TUBITAK Grant No. TBAG-1085.

¹D. M. Eigler and E. K. Schweizer, *Nature* **344**, 524 (1990).

²L. J. Whitman, J. A. Stroscio, R. A. Dragoset, and R. J. Celotta, *Science* **251**, 1206 (1991).

³I.-W. Lyo and P. Avouris, *J. Chem. Phys.* **93**, 4479 (1990); *Science* **253**, 173 (1991).

⁴H. J. Mamin, P. H. Guethner, and D. Rugar, *Phys. Rev. Lett.* **65**, 2418 (1990).

⁵D. M. Eigler, C. P. Lutz, and W. E. Rudge, *Nature* **352**, 600 (1991).

⁶*Atomic and Nanometer-Scale Modification of Materials: Funda-*

- mentals and Applications*, edited by Phaedon Avouris (Kluwer Academic, Dordrecht, 1993).
- ⁷S. Ciraci and I. P. Batra, *Phys. Rev. B* **36**, 6194 (1987); E. Tekman and S. Ciraci, *ibid.* **40**, 10 286 (1989); S. Ciraci, in *Basic Concepts and Applications of Scanning Tunneling Microscopy and Related Techniques*, edited by H. Rohrer, N. Garcia, and J. Behm (Kluwer, Amsterdam, 1989), p. 119.
- ⁸S. Ciraci, A. Baratoff, and I. P. Batra, *Phys. Rev. B* **41**, 2763 (1990).
- ⁹R. Gomer, *IBM J. Res. Dev.* **30**, 426 (1986).
- ¹⁰S. Ciraci, E. Tekman, A. Baratoff, and I. P. Batra, *Phys. Rev. B* **46**, 10 411 (1992); S. Ciraci, in *Theory of Tip-Sample Interactions in Scanning Tunneling Microscopy III*, edited by R. Wiesendanger and H.-J. Güntherodt, Springer Series in Surface Science Vol. 29 (Springer, Berlin, 1993), p. 179.
- ¹¹A. Baratoff, S. Ciraci, and E. Stoll (unpublished).
- ¹²J. R. Cerda, P. L. de Andres, F. Flores, and R. Pérez, *Phys. Rev. B* **45**, 8721 (1992); X. Bouju, C. Joachim, C. Girard and P. Sautet, *ibid.* **47**, 7454 (1993).
- ¹³A. Buldum, S. Ciraci, and Ş. Erkoç, in *Forces in Scanning Probe Methods*, edited by H. J. Güntherodt, D. Anselmetti, and E. Meyer (Kluwer, Dordrecht, 1995), p. 149; *J. Phys. Condens. Matter* **7**, 8487 (1995).
- ¹⁴S. Gao, M. Persson, and B. I. Lundqvist, *Solid State Commun.* **84**, 271 (1992); *J. Electron. Spectrosc. Relat. Phenom.* **64/65**, 665 (1993).
- ¹⁵J. J. Sáenz and N. Garcia, *Phys. Rev. B* **47**, 7537 (1993).
- ¹⁶R. E. Walkup, D. M. Newns, and P. Avouris, *Phys. Rev. B* **48**, 1858 (1993).
- ¹⁷G. P. Salam, M. Persson, and R. E. Palmer, *Phys. Rev. B* **49**, 10 655 (1994).
- ¹⁸M. Brandbyge and P. Hedegård, *Phys. Rev. Lett.* **72**, 2919 (1994).
- ¹⁹J. A. Barker and C. T. Rettner, *J. Chem. Phys.* **97**, 5844 (1992).
- ²⁰J. E. Müller, *Phys. Rev. Lett.* **65**, 3021 (1990).
- ²¹N. D. Lang, *Phys. Rev. Lett.* **46**, 342 (1981).
- ²²S. Ishi and B. Viswanathan, *Thin Solid Films* **201**, 373 (1991).
- ²³R. Pérez, F. J. Garcia-Vidal, P. L. de Andrés, and F. Flores, *Surf. Sci.* **307-309**, 704 (1994); J. R. Cerda, F. Flores, P. L. de Andrés, and P. M. Echenique, *Nuovo Cimento* **15D**, 451 (1993).
- ²⁴Y. C. Chen, J. E. Cunningham, and C. P. Flynn, *Phys. Rev. B* **30**, 7317 (1984).
- ²⁵J. Topping, *Proc. R. Soc. London Ser. A* **114**, 67 (1927).
- ²⁶D. M. Eigler, P. S. Weiss, E. K. Schweizer, and N. D. Lang, *Phys. Rev. Lett.* **66**, 1189 (1991).
- ²⁷B. Gumhalter and D. M. Newns, *Phys. Lett.* **57A**, 423 (1976).
- ²⁸K. Wandelt and B. Gumhalter, *Surf. Sci.* **140**, 355 (1984).
- ²⁹A. Buldum, M.S. thesis, Bilkent University, 1994.
- ³⁰D. M. Newns, *Phys. Rev.* **178**, 1123 (1969).
- ³¹P. W. Anderson, *Phys. Rev.* **124**, 41 (1961).
- ³²F. Herman and S. Skillman, *Atomic Structure Calculations*, (Prentice-Hall, Englewood Cliffs, NJ, 1963).
- ³³G. Schönhense, *Appl. Phys. A* **41**, 39 (1986).
- ³⁴N. D. Lang and W. Kohn, *Phys. Rev. B* **7**, 3541 (1973); calculations based on the nonlocal exchange-correlation approximation in S. Ossicini and C. M. Bertoni, *Europhys. Lett.* **1**, 661 (1986) yield relatively smaller values for d_i .
- ³⁵B. N. J. Persson and R. Ryberg, *Phys. Rev. B* **32**, 3586 (1985); J. A. Leiro and M. Persson, *Surf. Sci.* **207**, 473 (1989).
- ³⁶H. B. Huntington and A. R. Grone, *J. Phys. Chem. Solids* **20**, 76 (1961); V. B. Fiks, *Fiz. Tverd. Tela (Leningrad)* **1**, 16 (1959) [*Sov. Phys. Solid State* **1**, 12 (1959)].
- ³⁷K. S. Ralls, D. C. Ralph, and R. A. Buhrman, *Phys. Rev. B* **40**, 11 561 (1989).
- ³⁸J. Kirtley, in *Tunneling Spectroscopy*, edited by P. K. Hansma (Plenum, New York, 1982); D. J. Scalapino and S. M. Marcus, *Phys. Rev. Lett.* **18**, 459 (1967).
- ³⁹B. N. J. Persson and J. E. Demuth, *Solid State Commun.* **57**, 769 (1986); A. Baratoff and B. N. J. Persson, *J. Vac. Sci. Technol. A* **6**, 331 (1988).
- ⁴⁰J. W. Gadzuk, *Phys. Rev. B* **44**, 13 466 (1991).
- ⁴¹N. G. van Kampen, *Stochastic Process in Chemistry and Physics*, (North-Holland, Amsterdam, 1992).